

Specific Features of the Optical and Electrical Properties of Polycrystalline CdTe Films Grown by the Thermal Evaporation Method

V. V. Brus^a, M. N. Solovan^{a,*}, E. V. Maistruk^a, I. P. Kozyarskii^a,
P. D. Maryanchuk^a, K. S. Ulyanytsky^a, and J. Rappich^b

^a Yuriy Fedkovych Chernivtsi National University, ul. Kotsjubynskiyi 2, Chernivtsi, 58012 Ukraine

* e-mail: m.solovan@chnu.edu.ua

^b Helmholtz-Zentrum Berlin für Materialien und Energie, Hahn-Meitner-Platz 1, Berlin, 14109 Germany

Received January 16, 2014; in final form April 16, 2014

Abstract—The results of studying the physical properties of thin CdTe films obtained by the thermal evaporation method have been presented. The optical constants and the band gap of the films under study have been determined ($E_g = 1.46$ eV). It has been established based on the investigation of optical properties and the Raman spectrum of the films that they possess high structural quality. The activation energy of the electrical conductivity of CdTe films has been determined: $E_a = 0.039$ eV. The measured spectral dependences of the impedance of CdTe thin films are characteristic of the inhomogeneous medium with two time constants: $\tau_{gb} = R_{gb}C_{gb} = 1/\omega_{gb} = 1.62 \times 10^{-3}$ s and $\tau_g = R_gC_g = 1/\omega_g = 9.1 \times 10^{-7}$ s for grain boundaries and grains, respectively.

DOI: 10.1134/S1063783414100072

1. INTRODUCTION

Cadmium telluride (CdTe) is one of most promising materials for the fabrication of solar cells in view of its high absorption coefficient ($>10^5$ cm⁻¹) and optimal band gap (1.5 eV). Currently, about ten methods of the fabrication of thin CdTe films are developed [1–3].

Cadmium telluride films have been for a long time used to develop heterostructure-based solar cells. An increase in efficiency of such elements is directly associated with an increase in quality of starting materials for the development of heterostructures, as well as with the understanding of their physical properties.

There are many publications on the investigation of optical and electrical properties of CdTe films [2–11]. However, there are few results of complex experimental investigations of spectral dependences of fundamental optical constants. There are also few data on the dc and ac electrical properties of high-quality CdTe films grown by the thermal evaporation method—one of cheapest. Therefore, our investigations are very important for the further development of highly efficient devices based on heterojunctions for electronics and solar power engineering [12–14].

2. SAMPLE PREPARATION AND EXPERIMENTAL TECHNIQUE

The CdTe films were deposited on preliminarily cleaned glass substrates $24 \times 24 \times 0.15$ mm in size using a UVN-70 vacuum installation with the thermal evap-

oration from a tungsten crucible in a quasi-closed volume. We used *p*-CdTe crystals grown by the Bridgman method at low cadmium vapor pressures ($P_{Cd} = 0.02$ atm) as the material for the film growth. The room-temperature (295 K) electrical conductivity and charge carrier concentration were $\sigma = 8.9 \times 10^{-2}$ Ω⁻¹ cm⁻¹ and $p = 7.2 \times 10^{15}$ cm⁻³, respectively.

Before the deposition, the vacuum chamber was pumped to a residual pressure of 5×10^{-3} Pa. The deposition was performed for ~10 min at a substrate temperature of 570 K.

The samples for measuring electrical resistance had two current ohmic contacts, which were formed by deposition of molybdenum through a mask. To form the ohmic contacts to the *p*-CdTe film, the contact area was bombarded by argon ions [15] in the vacuum chamber to create the *p*⁺-region due to the formation of cadmium vacancies. After the surface was treated, a molybdenum layer was deposited on it by magnetron sputtering at a substrate temperature of ~400 K [15].

The temperature dependence of the electrical resistance was measured in the temperature range $T = 300$ – 420 K. Film parameters can vary during measuring the temperature dependences due to irreversible processes; therefore, investigations were performed both for heating and for cooling.

The spectral dependence of the impedance of the films under study was measured using a COMPACTSTAT.e: Portable Electrochemical Interface & Impedance Analyser (IVIUM Technologies).

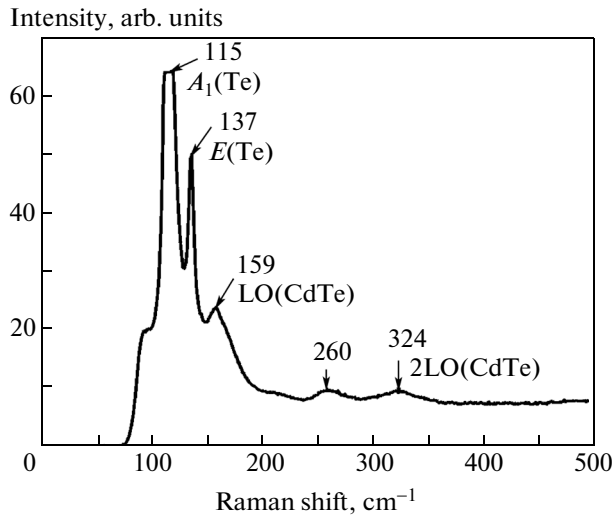


Fig. 1. Raman spectrum of CdTe thin films.

Transmission spectra of thin films were recorded on an SF-2000 spectrophotometer. Experimental curves were measured in the wavelength range of 200–1100 nm with a step of 1 nm.

The Raman spectra were measured using a LabRAM Raman microscope at a laser radiation wavelength of 632.82 nm.

3. RESULTS AND DISCUSSION

3.1. Structural Properties

Figure 1 shows a typical Raman spectrum for CdTe samples with inclusions of Te clusters. Modes A_1 (115 cm^{-1}) and E (137 cm^{-1}) of tellurium as well as weak first-order LO modes of cadmium telluride (159 cm^{-1}) and second-order 2LO modes of CdTe (324 cm^{-1}) are clearly seen in the spectrum. The position of peaks agrees well with the results reported in [16, 17]. A peak at 260 cm^{-1} is caused by vibrations of excess tellurium atoms [18]. The presence of excess tellurium atoms is caused by the formation of cadmium vacancies due to the use of the low-resistivity p -type base material to obtain the films. The presence of pronounced peaks indicates high structural quality of the films. Such films can be single-crystalline or polycrystalline with large crystallites.

3.2. Optical Properties

Figure 2 shows the transmission spectrum of CdTe films. Periodic peaks and valleys caused by interference phenomena are observed, which also indicates high structural quality of such films.

Optical properties of thin films (refractive index $n(\lambda)$, absorption coefficient $\alpha(\lambda)$, and extinction coefficient $k(\lambda)$) and thickness d can be determined from the transmission spectrum with interference phenom-

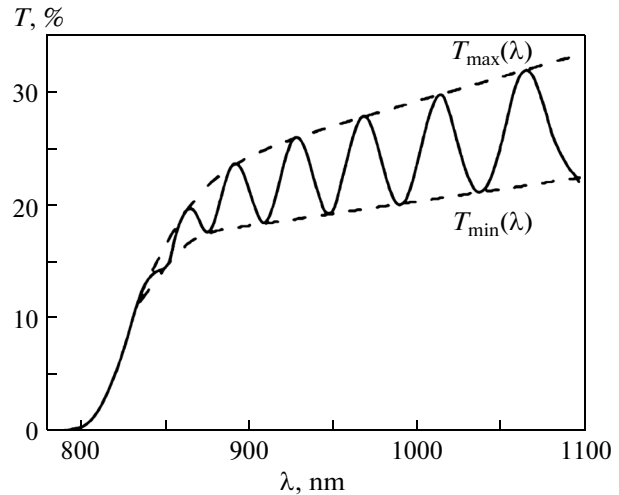


Fig. 2. Transmission spectrum of the CdTe thin film deposited on a glass substrate with convert curves for interference maxima $T_{\max}(\lambda)$ and minima $T_{\min}(\lambda)$.

ena using the convert method [19–22]. This method can be used under the condition of weak absorption by a thin film and full transparency of the substrate, which is much thicker than the film. Such conditions are fulfilled in our study.

Convert curves $T_{\max}(\lambda)$ and $T_{\min}(\lambda)$ are the basis of the convert method. They are formed using parabolic extrapolation of experimental points, which correspond to the location of interference maxima and minima in the transmission spectra (Fig. 2).

From the obtained convert curves, we can determine the dependence of the refractive index on the wavelength $n(\lambda)$ of thin films under study using the equation

$$n(\lambda) = \left[\left(\frac{2n_s(T_{\max} - T_{\min})}{T_{\max}T_{\min}} + \frac{n_s^2 + 1}{2} \right) \times \sqrt{\left(\frac{2n_s(T_{\max} - T_{\min})}{T_{\max}T_{\min}} + \frac{n_s^2 + 1}{2} \right)^2 - n_s^2} \right]^{\frac{1}{2}}, \quad (1)$$

where T_{\max} and T_{\min} are the functions of wavelength λ and n_s is the substrate refractive index, which is determined by the following expression:

$$n_s = \frac{1}{T_s} - \sqrt{\frac{1}{T_s^2} - 1}. \quad (2)$$

Here, T_s is the substrate transmittance, which is almost constant in the transparency region.

For the used glass substrates, we have $T_s = 0.91$; therefore, we derive from Eq. (2) that $n_s = 1.554$.

It should be noted that Eq. (1) can be used only within the interference band. The refractive index outside of this region can be determined by extrapolation of calculated data [20].

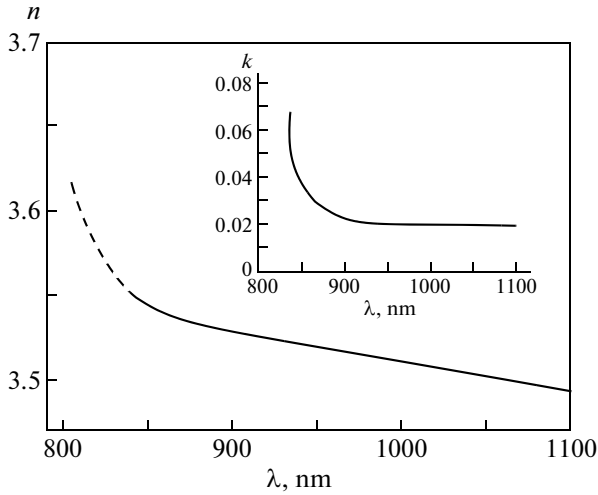


Fig. 3. Wavelength dependence of the refractive index of CdTe thin films. The inset shows the wavelength dependence of the extinction coefficient for the same films.

It is seen from Fig. 3 that the refractive indices $n(\lambda)$ of CdTe films calculated by Eq. (1) decrease as the wavelength increases. An abrupt increase in the refractive index at wavelengths $\lambda < 850$ nm is caused by a decrease in the transmittance near the self-absorption edge of cadmium telluride thin films.

To determine the thickness of the films under study, we can use the equation

$$d = \frac{A\lambda_1\lambda_2}{2[n(\lambda_1)\lambda_2 - n(\lambda_2\lambda_1)]}, \quad (3)$$

where λ_1 and λ_2 are wavelengths corresponding to neighboring extreme points in the transmission spectrum and $A = 1$ for two neighboring extrema of one type (max–max, min–min) and $A = 0.5$ for two neighboring extrema of opposite types (max–min, min–max). The average thickness of the CdTe film calculated by Eq. (3) is $3.585 \mu\text{m}$ for all combinations of extreme points.

The absorption coefficient $\alpha(\lambda)$ of CdTe films can be calculated using the equation

$$\alpha(\lambda) = \frac{1}{d} \ln \left[\frac{(n-1)(n-n_s)(\sqrt{T_{\max}/T_{\min}} + 1)}{(n+1)(n+n_s)(\sqrt{T_{\max}/T_{\min}} - 1)} \right], \quad (4)$$

where n , T_{\max} , and T_{\min} are functions of wavelength λ .

The absorption coefficient $\alpha(\lambda)$ is depicted in inset to Fig. 4. It is seen from Fig. 4 that the absorption coefficient abruptly increases in the vicinity of the self-absorption edge and smoothly decreases as wavelength increases.

The extinction coefficient can be easily determined using equations $k(\lambda) = \lambda\alpha(\lambda)/4\pi$. The extinction coefficient also abruptly increases in the vicinity of the self-absorption edge of the films under study (inset in

$$(\alpha h\nu)^2 \times 10^{-8}, \text{ cm}^{-2} \cdot \text{eV}^2$$

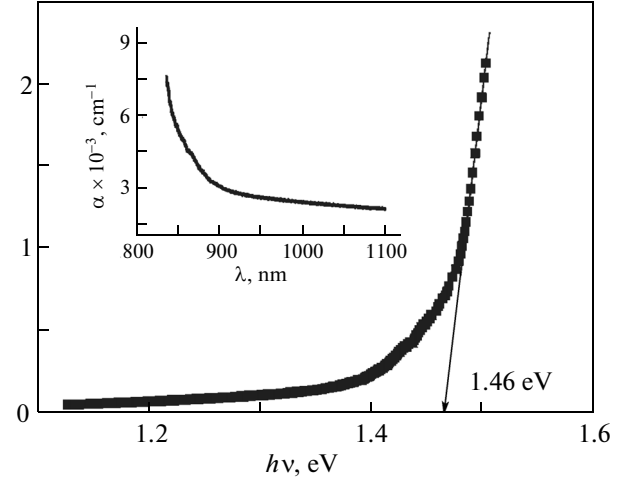


Fig. 4. Dependence $(\alpha h\nu)^2 = f(h\nu)$ for CdTe thin films. The inset shows the absorption spectrum of CdTe thin films.

Fig. 3). However, it is almost invariable in the transparency region ($\lambda > 900$ nm).

The convert method can be used only in the transparency region limits of a thin film. The following conditions are valid in a wavelength region near the self-absorption edge of CdTe films: strong absorption in the film material, a completely transparent substrate, and $n^2 \gg k^2$. Starting from the aforesaid, we can conclude that the absorption coefficient $\alpha(\lambda)$ (in the strong absorption region by the material of CdTe films) can be determined using the equation [23]

$$\alpha(\lambda) = \frac{1}{d} \ln \left[\frac{(1-R_1)(1-R_2)(1-R_{12})}{T} \right], \quad (5)$$

where T , R_1 , R_{12} , and R_2 are the functions of wavelength λ ; T is transmittance; and $R_1 = \left(\frac{n(\lambda)-1}{n(\lambda)+1} \right)^2$,

$R_{12} = \left(\frac{n_s - n(\lambda)}{n_s + n(\lambda)} \right)^2$, and $R_2 = \left(\frac{1-n_s}{1+n_s} \right)^2$ are the coefficients of reflection from the air–film, film–substrate, and substrate–air interfaces, respectively.

We established that the absorption coefficient of the CdTe film in the self-absorption region is described well by the following dependence:

$$\alpha(h\nu) = A(h\nu - E_g)^{1/2}, \quad (6)$$

where A is a certain coefficient, which depends on effective masses of charge carriers. Such dependence $\alpha(h\nu)$ indicates that the material of the CdTe film deposited by the thermal evaporation method is the direct-gap semiconductor. We determined the band gap of the CdTe thin film ($E_g = 1.46$ eV) by extrapolation of the linear segment of dependence $(\alpha h\nu)^2 = f(h\nu)$ to the intersection with energy axis $h\nu$ (Fig. 4).

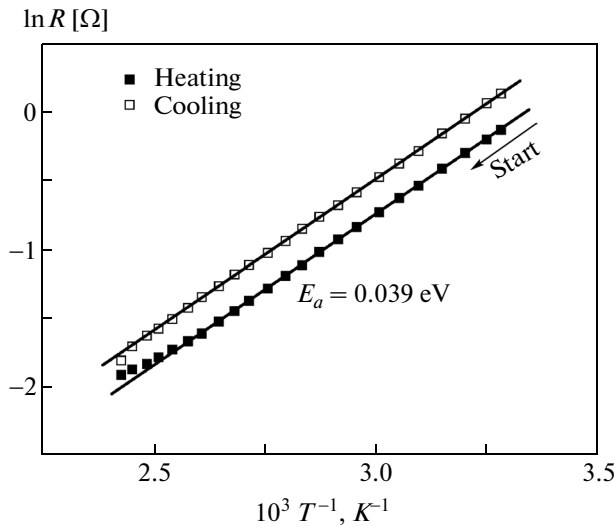


Fig. 5. Temperature dependence of the electrical resistance of CdTe films upon their heating and cooling.

3.3. Electrical Properties

The temperature dependence of the electrical resistance of freshly deposited CdTe films for two directions of varying the temperature is presented in Fig. 5. It is seen that variations occur in films due to heating, which lead to an increase in their resistance. The activation energy determined by straight-linear segments of experimental dependences $R = f(T)$ for the CdTe film is 0.039 eV, which agrees well with the depth of acceptor levels formed by cadmium vacancies ($E_v + 0.05$ eV) [24, 25]. The presence of the latter is confirmed by the excess of tellurium, which is observed in the Raman spectra (Fig. 1).

It should be noted that the activation energy did not varied due to heating, and only the film resistance increased. An increase in resistance is caused by a decrease in the number of cadmium vacancies due to film annealing during the measurement.

3.4. Impedance Spectroscopy

The spectral dependences of real Z' and imaginary Z'' parts of the impedance of the film under study are depicted in Figs. 6 and 7, respectively.

Measured spectral dependences of impedance (two steps and two minima in dependences for Z' and Z'' , respectively) of the CdTe thin film are characteristic of an inhomogeneous medium with two time constants, which is simulated in frameworks of the equivalent circuit depicted in inset to Fig. 6 [26, 27]. Segments $R_g C_g$ and $R_{gb} C_{gb}$ qualitatively take into account the influence of connected in series grains and grain boundaries on the conditions of charge transfer through a thin film under study. The influence of grain boundaries dominates in a low-frequency region, while the influence of grains dominates in a high-frequency

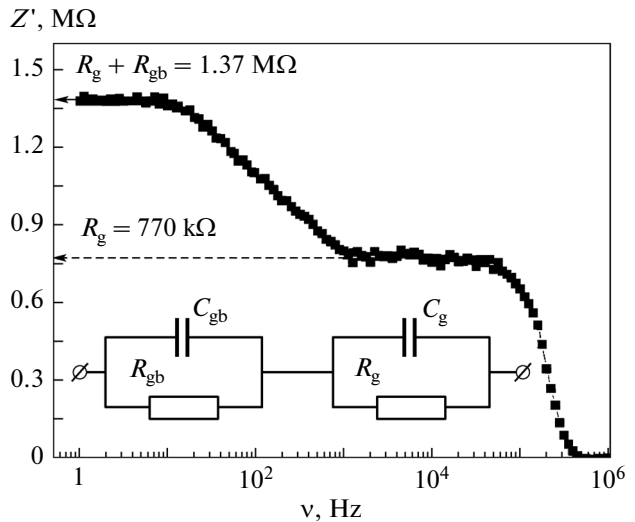


Fig. 6. Spectral dependence of the real part of the measured impedance Z' of the CdTe thin film.

region [27]. Taking into account the selected equivalent circuit (inset in Fig. 6), the spectral dependence of measured impedance Z can be quantitatively described using the following expression [26, 27]:

$$Z = \left[\frac{R_{gb}}{1 + \omega^2 C_{gb}^2 R_{gb}^2} + \frac{R_g}{1 + \omega^2 C_g^2 R_g^2} \right] - i \left[\frac{\omega C_{gb} R_{gb}^2}{1 + \omega^2 C_{gb}^2 R_{gb}^2} + \frac{\omega C_g R_g^2}{1 + \omega^2 C_g^2 R_g^2} \right] = Z' + iZ'' \tag{7}$$

where $\omega = 2\pi\nu$ is a cyclic frequency of a low-amplitude variable signal (10 mV); R_{gb} and R_g are resistances of grain boundaries and crystallites, respectively; and C_{gb} and C_g are capacities of grain boundaries and crystallites, respectively.

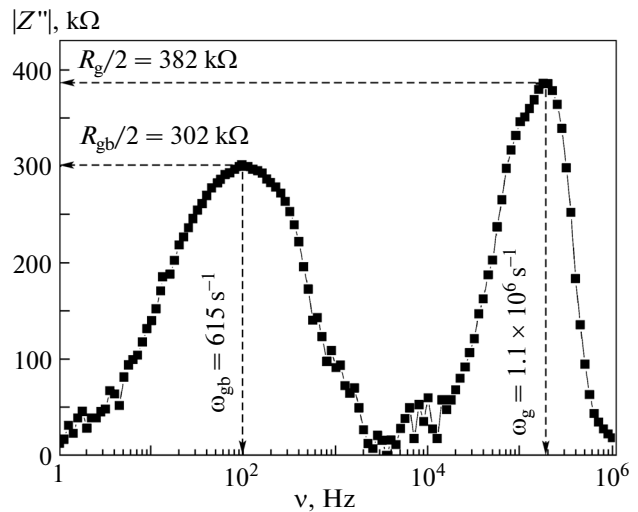


Fig. 7. Spectral dependence of the modulus of the imaginary part of the measured impedance Z'' of the CdTe thin film.

Using expression (7), we can show that resistances R_{gb} and R_g are determined by extrapolation of corresponding horizontal segments of spectral dependence Z' or are found from corresponding extreme values of spectral dependences Z'' as shown in Figs. 6 and 7, respectively [28–30]. Positions of minima of the spectral dependence for the impedance imaginary part Z'' (Fig. 7) determine time constants for the corresponding chain of the equivalent circuit and, therefore, for the electric component of the material of the CdTe thin film [28]: time constant of grain boundaries $\tau_{gb} = R_{gb}C_{gb} = 1/\omega_{gb} = 1.62 \times 10^{-3}$ s, and time constant of grains $\tau_g = R_gC_g = 1/\omega_g = 9.1 \times 10^{-7}$ s. From here, we can easily determine the values of capacities $C_{gb} = 2.68 \times 10^{-9}$ F and $C_g = 1.18 \times 10^{-12}$ F.

4. CONCLUSIONS

The CdTe thin films are grown on glass substrates by the thermal evaporation of the powder of p -CdTe crystals.

The investigation of the Raman spectrum of the films shows the presence of pronounced peaks, which indicate high structural quality of films as well as show the presence of excess tellurium atoms in films. The presence of excess tellurium atoms is possibly caused by the formation of cadmium vacancies in a low-ohmic base p -type material, which was used to prepare the films.

Using the convert method, we determined optical constants of CdTe thin films (refractive index $n(\lambda)$, absorption coefficient $\alpha(\lambda)$, and extinction coefficient $k(\lambda)$) as a function of the wavelength, as well as the band gap of the films under study: $E_g = 1.46$ eV.

We measured the temperature dependence of the electrical resistance of the films under study $R = f(T)$. Activation energy of 0.039 eV for CdTe films is determined in the temperature range of 300 K $< T <$ 420 K, which agrees well with the depth of acceptor levels formed by cadmium vacancies ($E_v + 0.05$ eV).

The measured spectral dependences of the impedance of the CdTe thin film are characteristic of the inhomogeneous medium with two time constants ($\tau_{gb} = R_{gb}C_{gb} = 1/\omega_{gb} = 1.62 \times 10^{-3}$ s and $\tau_g = R_gC_g = 1/\omega_g = 9.1 \times 10^{-7}$ s), which quantitatively take into account the influence of connected in series grain boundaries and crystallites, respectively, on the conditions of charge transfer through the thin film under study.

REFERENCES

1. T. L. Chu and S. S. Chu, *Solid State Electron.* **38**, 533 (1995).
2. S. Chandra, S. Tripura Sundari, G. Raghavan, and A. K. Tyagi, *J. Phys. D: Appl. Phys.* **36**, 2121 (2003).
3. H. R. Moutinho, F. S. Hasoon, F. Abulfotuh, and L. L. Kazmerski, *J. Vac. Sci. Technol., A* **13**, 2877 (1995).
4. G. K. Padam and G. L. Malhotra, *Mater. Res. Bull.* **24**, 595 (1989).
5. A. Gupta, V. Parikh, and A. D. Compaan, *Sol. Energy Mater. Sol. Cells* **90**, 2263 (2006).
6. T. M. Razykov, G. Contreras-Puente, G. C. Chornokur, M. Dybjec, Yu. Emirov, B. Ergashev, C. S. Ferekides, A. Hubbimov, B. Ikramov, K. M. Kouchkarov, X. Mathew, D. Morel, S. Ostapenko, E. Sanchez-Meza, E. Stefanakos, H. M. Upadhyaya, O. Vigil-Galan, and Yu. V. Vorobiev, *Sol. Energy* **83**, 90 (2009).
7. S. Sivananthan, X. Chu, J. Reno, and J. P. Faurie, *J. Appl. Phys.* **60**, 1359 (1986).
8. M. C. Nuss, D. W. Kisker, P. R. Smith, and T. E. Harvey, *Appl. Phys. Lett.* **54**, 57 (1989).
9. X. Mathew and P. J. Sebastian, *Sol. Energy Mater. Sol. Cells* **59**, 85 (1999).
10. D. Lincot, A. Kampmann, B. Mokili, J. Vedel, R. Cortes, and M. Froment, *Appl. Phys. Lett.* **67**, 2355 (1995).
11. I. Spinulescu-Carnaru, *Phys. Status Solidi B* **15**, 761 (1966).
12. M. M. Solovan, V. V. Brus, and P. D. Maryanchuk, *Semiconductors* **47** (9), 1174 (2013).
13. M. N. Solovan, V. V. Brus, and P. D. Maryanchuk, *Semiconductors* **48** (2), 219 (2014).
14. V. V. Brus, *Sol. Energy* **86**, 1600 (2012).
15. J. P. Punpon, *Solid State Electron.* **28**, 689 (1985).
16. S. Jimenez-Sandoval, *Microelectron. J.* **31**, 419 (2000).
17. M. M. Solovan, V. V. Brus, P. D. Maryanchuk, M. I. Ilashchuk, J. Rappich, N. Nickel, and S. L. Abashin, *Semicond. Sci. Technol.* **29**, 015007 (2014).
18. R. Ochoa-Landirn, O. Vigil-Galan, Y. V. Vorobiev, and R. Ramirez-Bon, *Sol. Energy* **83**, 134 (2009).
19. R. Swanepoel, *J. Phys. E: Sci. Instrum* **16**, 1214 (1983).
20. J. Sanchez-Gonzalez, A. Diaz-Parralejo, A. L. Ortiz, and F. Guiberteau, *Appl. Surf. Sci.* **252**, 6013 (2006).
21. S. Ilican, M. Gaglar, and Y. Gaglar, *Mater. Sci. Pol.* **25**, 709 (2007).
22. V. V. Brus, Z. D. Kovalyuk, and P. D. Maryanchuk, *Tech. Phys.* **57** (8), 1148 (2012).
23. Yu. I. Ukhanov, *Optical Properties of Semiconductors* (Nauka, Moscow, 1977) [in Russian].
24. K. Zanio, *Semiconductors and Semimetals* (Academic, New York, 1978).
25. V. V. Brus, M. I. Ilashchuk, Z. D. Kovalyuk, P. D. Maryanchuk, and K. S. Ulyanytsky, *Semicond. Sci. Technol.* **26**, 125006 (2011).
26. M. B. Ortuno-Lopez, J. J. Valenzuela-Jauregui, R. Ramirez-Bon, E. Prokhorov, and J. Gonzalez-Hernandez, *J. Phys. Chem. Solids* **63**, 665 (2002).
27. A. Azan, A. S. Ahmed, M. Charman, and A. H. Naqvi, *J. Appl. Phys.* **108**, 094329 (2010).
28. V. V. Brus, *Semiconductors* **46** (8), 1012 (2012).
29. V. V. Brus, *Semicond. Sci. Technol.* **27**, 035024 (2012).
30. V. V. Brus, *Semicond. Sci. Technol.* **28**, 025013 (2013).

Translated by N. Korovin